The Impact of Built-Up Area On Land Surface Temperature Derived From Cloud-Computing Landsat 8 Imagery

1st Rika Hernawati
Geodetics Engineering
Institut Teknologi Nasional
Bandung, Indonesia
rikah@itenas.ac.id

2nd Soni Darmawan
Geodetics Engineering
Institut Teknologi Nasional
Bandung, Indonesia
soni_darmawan@itenas.ac.id

3rd Derry Cahyanto
Geodetics Engineering
Institut Teknologi Nasional
Bandung, Indonesia
chahyantoodery@gmail.com

***Abstract*— Urbanization is needed to ensure a higher quality of life for the rapidly growing population worldwide. Changing the land surface is a significant effect of growth and causes an increase in the land surface temperature (LST). This research used remote sensing techniques to evaluate the impact between built-up area and LST in Bandung City, Indonesia in 2014 and 2019. The methodology includes data collection derived from Landsat 8 imagery, pre-processing, calculated the value of built-up area generated through the NDBI algorithm based on cloud-computing platform Google Earth Engine (GEE). The result showd the distribution of LST and density of built-up was increased from 2014 to 2019. The density of built-up had increased by 4.47 %, and the density of high buildings had increased by 0.06 %, The coefficient of determination R^2 between NDBI and LST in 2014 was 0.82 and 0.84 in 2019, which means that the potential of the built-up density to describe the surface temperature was 82.4 % in 2014 and 84.2 % in 2019. It can be concluded that the NDBI building density value and the LST soil surface temperature value have a very strong correlation.**

Keywords—Built-up, NDBI, LST, Landsat, Cloud-computing

I. Introduction

Bandung City is one of the largest cities in Indonesia with a density of population due to its strategic location and the economic center of West Java. The growth in population per year results in improvements in land use and a decrease in green open space (RTH). The area of green open space is 30% of the area (Law of the Republic of Indonesia No 26 of 2007), but in fact, many places can not make this happen [1]. Due to climate fluctuations in Bandung, there is a disparity between land-use changes, built-up area and green open space. Parameters should be used to realize the temperature variations are the ground surface temperature (LST) [2]. LST is an important parameter in the study of thermal and urban behavior [3]. The rise and fall of LST in temperatures below the atmospheric layer is an important element in the knowledge of surface radiation [4]. Remote sensing technologies can be used to identify the density of built-up land use. Several indices for extracting characteristics of interest from satellite imagery have been established [5]. That would be the NDBI (Normal Difference Built-Up Index) method [2], [4], [6]. Several latest research assess the LST-NDBI correlation of different types of LULC in the tropical climate [7]–[11]. The Normalized Built-up Difference Index (NDBI) is an important spectral index that correlates significantly with the LST [7].

Google Earth Engine (GEE) has been widely used in recent years for global-scale applications such as global forest cover transition characterization; forest growth, degradation, crop yields, and gain from 2000 using large Landsat scene collections [12]. Other studies have verified the flexibility of combining different sources of temporal satellite imagery data and the automatic classification procedures for vegetation and land cover mapping using GEE [12], [13]. Previously, the implementation of the LST algorithm and the computation of spectral indices on the GEE platform have opened up opportunities for online storage and analysis of all available Landsat data in a cloud-based environment with a simple-to-use application programming interface (API) [12], [14]. We applied the LST and NDBI derived from Landsat 8 in 2014 and 2019 to assess the impact of built-up area on LST in Bandung, Indonesia using cloud-computing GEE platform.

II. Material and Method

A. Study Area

Bandung is the capital of West Java province (Figure 1), located about 180 kilometers (110 mi) southeast of Jakarta 6° 54' 53.5104" S and 107° 36' 29.6568" E third-largest city in Indonesia. Its elevation is 768 meters (2,520 ft) above sea level and is surrounded by up to 2,400 meters (7,900 feet) high Late Tertiary and Quaternary volcanic terrain [15]. Since Bandung is located only about 90 miles away from Jakarta, it is possible to say that the two large cities are heavily interconnected and have similar cultures of urban life.

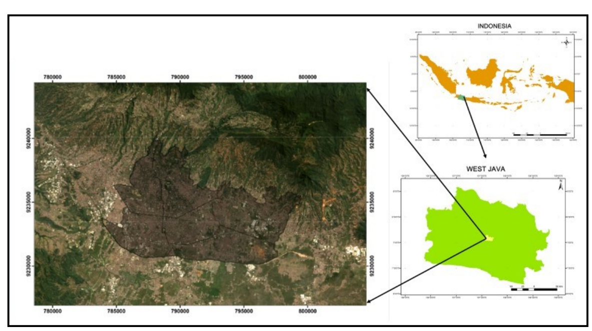

Fig 1. Study Area of Bandung.

The climate of the area is severely subtropical. However, the city of Bandung can be characterized by having less hot and less humid summertime than the climatic conditions of the other large and small cities and towns located close to the ocean's waters. Bandung experiences tropical monsoon climate (*Am*) according to Köppen climate classification as the driest month precipitation total is below 60 millimeters (2.4 in), bordering with subtropical highland climate (*Cfb*). The wettest month is February with 255.0 millimeters (10.04 in), while the driest month is September with a total of 50.0 millimeters (1.97 in). The average temperature throughout the year tends to be cooler than most of Indonesia's due to the altitude influence. The average temperature throughout the year only has little variation due to its location near the equator.

B. Methodology.

The methodology used in this analysis involves data sources, geometric corrections and radiometric corrections, which are the pre-processing steps needed for Landsat images, and processing requires the collection of surface temperature (LST), the NDBI evaluation and the determination of the relationship between NDBI and LST.

Band 6 and Band 5 of the satellite imagery were processed to obtain the built-up index, while Band 4 and Band 5 of the data were processed for NDVI analysis. Thermal band TIRS (Band 10) was analyzed for surface temperature recovery. In the following paragraphs, we discussed the full process of extracting these features from satellite data using the GEE cloud computing platform.

1) Data.

The data was extracted from Landsat-8 images acquisition collected in separate seasons, Rainy 13 September 2014 and summer 22 May 2019. showed in Table 1 and ancillary data from topographic maps Bandung. The images were obtained from the US Geological Survey (USGS) Landsat series of Earth Observation satellites available in GEE. All images were in a geographic latitude/longitude projection and datum World Geodetic System 1984 (WGS84).

TABLE 1. Landsat 8 Data Acquisition

Date of acquisition	Source	Path/Row
13 September 2014	USGS	122/65
22 May 2019	USGS	122/65

2) Data Processing

Briefly, the radiance values derived were used to calculate at satellite brightness temperature, that is, black body temperature followed by a correction for spectral emissivity according to the landscape [16]. LST distribution with band 10 (Landsat 8), and top of atmosphere brightness temperature values have been represented in Kelvin for each of the study areas [17].

The digital numbers (DN) of TIRS and OLI bands were converted to spectral radiance and top of atmosphere (TOA) planetary reflectance to preprocess the satellite images. The formula to convert DN to radiance below was used [18]:

$$L_\lambda = M_L Qcal + A9_L$$

Where L_λ = ToA spectral radiance, *ML* = band-specific multiplicative rescaling factor from the metadata, *Qcal* = quantized and calibrated standard product pixel values (DN), and *AL* = band- specific additive rescaling factor from the metadata.

The NDVI is computed by TOA planetary spectral reflectance, with solar angle correction. The DNs are converted to TOA planetary reflectance by the below equation [19]:

$$\rho\lambda = {}'\rho\lambda / \sin\theta = (Mp * Qcal + Ap)/ \sin\theta$$

where $\rho\lambda$ and $'\rho\lambda$ are TOA planetary spectral reflectance with and without solar angle correction (unitless), *Mp* is reflectance multiplicative scaling factor, *Ap* is reflectance additive scaling factor, and θ is solar elevation angle. *ML, AL, Mp, Ap*, and θ parameters in Equations is extracted from the metadata file, which is downloaded with satellite images from the USGS EarthExplorer.

a) NDVI Calculation

After conversion of the DN to reflectance, the normalized difference vegetation index (NDVI) forthe red and near infrared (NIR) bands was calculated by the following equation [20]:

$$NDVI = \frac{\rho NIR - \rho Red}{\rho NIR + \rho Red}$$

The index is used based on the rationale that vegetation reacts to the absorption and reflection of red and near-infrared lights. NDVI values range from − 1 to 1. A value of zero indicates the presence of urban areas while a negative value is an indication of a water body. A positive value closer to one indicates the presence of green cover [21], [22].

b) LST Calculation

In this research, the mono-window algorithm has been applied to retrieve LST from multi-temporal Landsat satellite imagery [8][2]. Ground emissivity, atmospheric transmittance, and sufficient mean atmospheric temperature these three parameters are needed to determine the LST using a mono-window algorithm. After the extraction process in (1) equation, conversion of spectral radiance (L_λ) to brightness temperatures (TB) corrections according to the following equation [3]:

$$T_B = \frac{K2}{\ln\left(\frac{K1}{L\lambda}\right)+1} - 273$$

where T_B is brightness temperature (°C), *K1* and *K2* stand for the band-specific thermal conversion constant from the metadata, $L\lambda$ is top of atmospheric spectral radiance. For the Conversion of sensor temperature to celsius, the absolute zero value was added to radiant temperature [3], [23].

The absolute temperature or Land surface temperature (LST) was estimated from average brightness temperature acquired from band 10 and band 11 of the Landsat 8 TIRS

data, the wavelength of emitted radiance, land surface emissivity, and constant value P. Land surface emissivity was calculated from the vegetation fraction which, in turn, derived from NDVI value range. The absolute temperature was calculated according to the method as employed by (Latif and Kamsan 2017), while the Landsat visible and near-infrared bands were used for calculating the NDVI.
The vegetation index (Pv) was calculated according to the equation as described by [24]:

$$PV = \frac{NDVI - NDVI_{min}}{NDVI_{max} - NDVI_{min}}$$

where $NDVI_{min}$ represents minimum NDVI value indicating the presence of bare soil and $NDVI_{max}$ is maximum NDVI value indicating the presence of healthy vegetation [8].
While the Ground Emissivity (ε) and Emissivity-corrected values were calculated according to the following equations [25].

$$\varepsilon = 0.985Pv + 0.960\ (1-Pv) + 0.06Pv\ (1-Pv)$$

The emissivity corrected land surface temperatures (LST) was computed as following [26]

$$LST = \frac{Tb}{1+\left(\frac{\lambda Tb}{hc}\right) \ln \varepsilon}$$

Where *Tb* is *Temperature Brightness* (ºC), λ is wavelength of emitted radiance, ε is estimated land surface emissivity. Where ρ is the constant value obtained from Boltzman equation:

$$\rho = h\ x\ \frac{c}{\sigma};$$

where, *h* is Planck's constant (6.26 x 10^{-34}Jsec), *c* is Light velocity (2.998 x 10^{8} m s^{-1}), σ is Stefan-Boltzman constant (1.38 x 10^{-23} J K^{-1}).

Normal Difference Built-Up Index (NDBI). Value of building density index using band NIR and band SWIR on Landsat 8. The NDBI value in this study was obtained by adopting a calculation method from the equation below using GEE (figure 2) [27]:

$$NDBI = \frac{(SWIR-NIR)}{(SWIR+NIR)}$$

The parameters used in the algorithm are;
NIR = Near Infrared
SWIR = Short Wave Infrared

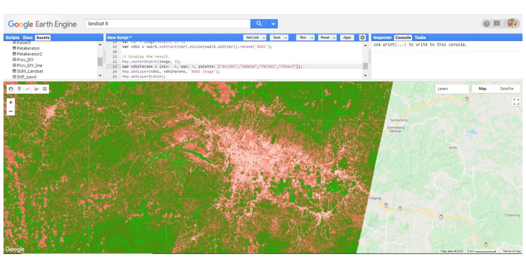

Fig 2. Calculating NDBI using Google Earth Engine

III. RESULT AND DISSCUSSION

A. Normal Difference Built-Up Index

The Normalized Difference Built-Up Index (NDBI) is a technique of approach that is mostly used in remote sensing to assess the area's building density value. The result of this study showing the distribution of Building Density Maps in 2014 and 2019 as shown as Figure 2. The NDBI value is between-1 and +1. According to Adeola et al (2020), the results of NDBI processing are classified into 4 classes, including non-building classes in the range-1-0, low building density classes in the range 0-0,(5)medium building density classes in the range 0.1-0.2, high building density classes in the range 0.2-0.3 [28].

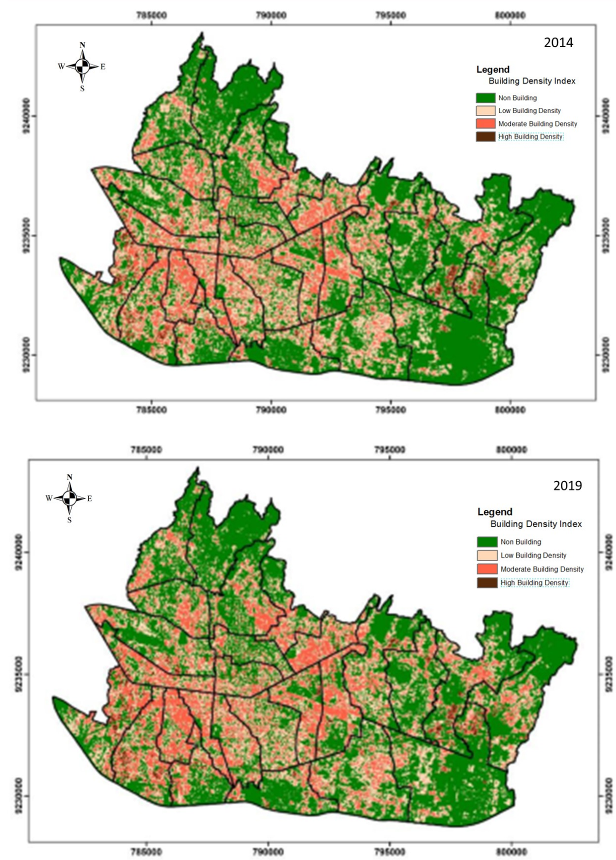

Fig 2. The Distribution of NDBI in 2014 and 2019

TABLE 2. NDBI Building Intensity Class Area in Bandung

NDBI Value	Area (Ha)		Changes (%)	The Area Changes (Districts)
	2014	2019		
-1 - 0	8611.6	8334.36	-1.7	- Cidadap - Rancasari - Bandung Kulon
0 – 0.1	5145.4	4668.75	-2.8	- Rancasari - Marga Cinta - Bandung Kulon - Cibiru - Bojongloa Kidul
0.1 – 0.2	2839.9	3581.55	4.47	- Bandung Wetan - Cibeunying Kidul - Sukajadi - Cicendo - Andir - Kiaracondong - Cibeunying Kaler
0.2 – 1	259.29	271.44	0.06	- Babakan Ciparay - Arcamanik - Ujung Berung - Cibiru - Bandung Kulon

Based on the results of the measurement of the NDBI area in Bandung City in 2014 and 2019, it is seen that there is an increasing trend in the density of buildings as defined in Table 2. Increased building density values typically exist in city centres such as Cibeunying Kidul, Cibeunying Kaler, Kiaracondong and other city centers. The non-building class and the low building density class display a lower average, which is inversely proportional to the medium building density class and the high building density class, which shows an increase. It can be assumed that the building density in Bandung City increased from 2014 to 2019, in order to further explain the effects of the measurement of the NDBI area, a frequency analysis showing the pattern can be seen in Figure 3.

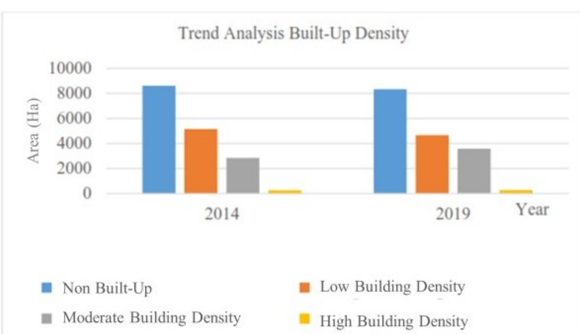

Fig 3. Trend Analysis of Built-Up area in 2014 and 2019

B. Land Surface Temperature

Land surface temperature (LST) is a method for estimating the temperature using thermal bands in Landsat images. The method used to calculate the value of the LST is a mono window since it requires only one thermal band. The soil surface temperature has a correlation that is determined by vegetation density, if the vegetation density is high, the surface temperature is low and preferable. The result of this study showing the distribution of Land Surface Temperature in 2014 and 2019 as shown as Figure 4.

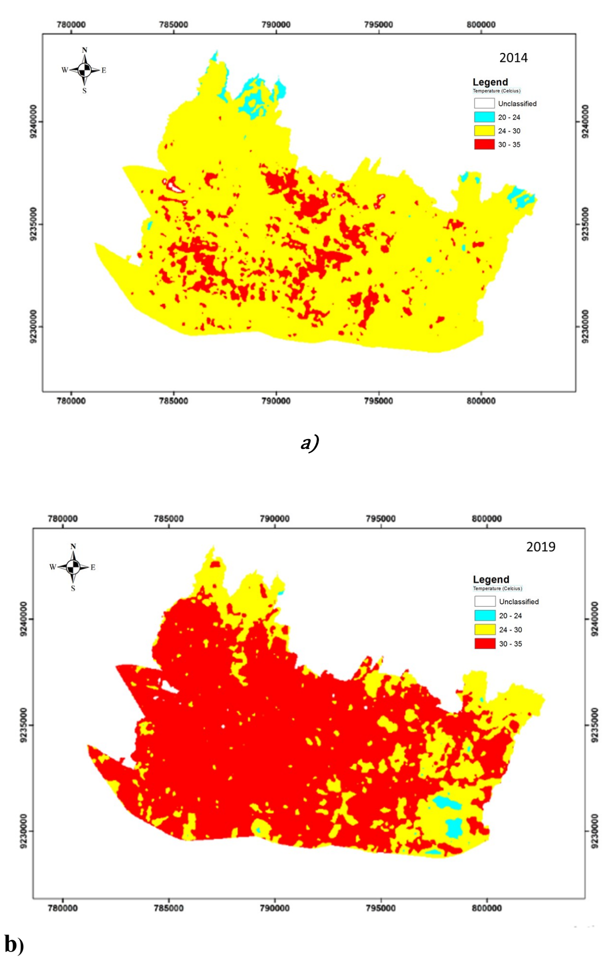

Fig 4. The Distribution of LST in a). 2014 and b). 2019

Based on the impact of the LST estimation of processing seen in Figure 4, it is shown that the dominant temperature in Bandung is different every year where the dominant temperature in 2014 is between 24°C and 30°C, whereas the dominant temperature in 2019 is between 30°C and 35°C. The minimum temperature of Bandung City produced during image processing in 2014 is 20.05°C and the maximum temperature is 31.99°C, while in 2019 the minimum temperature is 20.44°C and the maximum temperature is 35.13° C.

C. Correlation Analysis between NDBI and LST

Correlation is an analysis used to find out how much the strength of the relationship between two or more variables. Correlation analysis is done by taking a random sample with stratified method where this method was to select stratified samples to represent each surface temperature value.

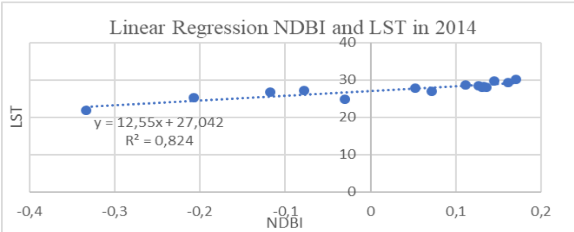

(a)

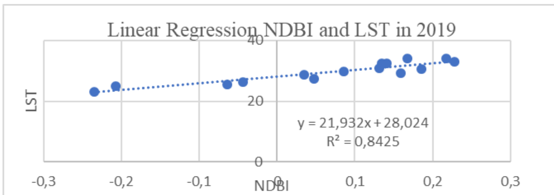

(b)

Figure 4. Linear Regression NDBI and LST in (a) 2014 and (c) 2019.

Results of the scatterplot show the regression coefficient value is positive, where the higher the level of the building density index, the surface temperature value of the ground will be higher too, and conversely if the level of the building density index in an area is low, its value from the surface temperature of the land in this area is low. The equation of the coefficient of determination in 2014 was 0.824 and 2016 was 0.9122, while in 2019 had a value 0.8425 thats means the effect of building density on surface temperature was 82.4% for 2014 and 84, 25% for 2019. According to Boediono (2001), the meaning of the correlation value if it shows the value of r = 0.90 <r <1.00 or -1.00 <r <-0.90, that's means has a very strong relationship [29]. It can be concluded that the NDBI building density value and the LST soil surface temperature value have a very strong correlation.

D. Validation of Buil-Up Density

Validation is needed to determine if the results of the analysis are the same as the actual conditions. Validation used google earth, a validation procedure only in 2019 as a sample to evaluate the accuracy of the processing data. The results of the image processing in 2019 showed that Bandung had an area of 16865.1 ha. The effects of of extensive built-up area was 8521.74 ha or 50.56% of the total area.

TABLE 3. The Accuracy of Built-Up area

Class	Field data *(Google Earth)*				Total Pixel	Procedure's Accuracy
	Non Built-Up	Low Building Density	Moderate Building Density	High Building Density		
Non Built-Up	30	0	0	0	30	100
Low Building Density	0	30	1	0	31	96.77
Moderate Building Density	0	0	28	2	30	93.33
High Building Density	0	0	1	28	29	96.55
Total Pixel	30	30	30	30		
User's Accuracy	100	100	93.33	93.33		

The results of the classification using the Area Of Interest (AOI) technique, the estimation is carried out to see the total precision, the value was 96.67% and the kappa was 96.42%. These data are compatible with the tolerance where the accuracy value of the kappa is accepted if it is greater than or equal to 85 % [30]. It can also be concluded that the results of the data processing are correct, even if there are certain improper samples.

IV. CONCLUSIONS

Based on the studies that have been conducted, it can be assumed that the building density has a very strong impact on the surface temperature in Bandung Region. Linear regression was used to assess the impact of building density on surface temperatures. The coefficient of determination R^2 between NDBI and LST in 2014 was 0.82 and 0.84 in 2019, which means that the potential of the built-up density to describe the surface temperature was 82.4 % in 2014 and 84.2 % in 2019 and the balance was explained by other factors beyond the variables in the regression equation. To figure it out how the relationship between the NDBI and the LST variables is required, the value of the correlation coefficient is called R. The value of the R was calculated from the value of the relationship R = 0.91 in 2014 and the value of the relationship R = 0.91 in 2019, which indicated a very strong correlation.

Distribution of surface temperature and density of built-up in Bandung Area in general, it increased from 2014 to 2019. The density of built-up had decreased by 4.47 %, and the density of high buildings had increased by 0.06 %, and the processing results showed that density changes occur in urban centers such as Astana Anyar District, Cibeunying Kidul, Cibeunying Kaler, Arcamanik and Kiaracondong.

The surface temperature in Bandung had increased significantly. 2014 showed that the dominant temperature was in 24°C -30°C, while in 30°C -35°C in 2014 it was located in urban areas such as Cibeunying Kaler, Cibeunying Kidul and Astana Anyar districts. The year 2019 showed that the dominant temperature in Bandung was in the 30°C -35°C, which was distributed almost throughout the city of Bandung, while the 20°C -24 °C and 24°C-30 ° C were in the suburbs of Bandung City, such as Cidadap, Rancasari and Cibiru districts.

ACKNOWLEDGMENT

In addition, the researcher would like to acknowledge the funding support from LPPM Itenas Bandung.

REFERENCES

[1] C. Werner, "Green Open Spaces in Indonesia cities: schisms between law and practice," no. February, 2015.

[2] Z. Qin, A. Karnieli, and P. Berliner, "A mono-window algorithm for retrieving land surface temperature from Landsat TM data and its application to the Israel-Egypt border region," *International Journal of Remote Sensing*, vol. 22, no. 18, pp. 3719–3746, 2001, doi: 10.1080/01431160010006971.

[3] J. Cristóbal, J. C. Jiménez-Muñoz, A. Prakash, C. Mattar, D. Skoković, and J. A. Sobrino, "An improved single-channel method to retrieve land surface temperature from the landsat-8 thermal band," *Remote Sensing*, vol. 10, no. 3, 2018, doi: 10.3390/rs10030431.

[4] J. A. Voogt, "Urban heat island," 2000.

[5] M. Myo Khine, Y. Y. Maw, K. Mi, and M. Win, "Change Analysis of Indices (Ndwi, Ndvi,Ndbi) for Mawlamyine City Area Using Google Earth Engine," *J. Myanmar Acad. Arts Sci*, vol. 5, no. 1, 2018.

[6] J. A. Voogt and T. R. Oke, "Thermal remote sensing of urban climates," *Remote Sensing of Environment*, vol. 86, no. 3, pp. 370–384, 2003, doi: 10.1016/S0034-4257(03)00079-8.

[7] S. Guha, H. Govil, N. Gill, and A. Dey, "A long-term seasonal

analysis on the relationship between LST and NDBI using Landsat data," *Quaternary International*, no. June, 2020, doi: 10.1016/j.quaint.2020.06.041.

[8] S. Guha, H. Govil, and P. Diwan, "Monitoring LST-NDVI Relationship Using Premonsoon Landsat Datasets," *Advances in Meteorology*, vol. 2020, no. 1, 2020, doi: 10.1155/2020/4539684.

[9] C. O. Wilson and Q. Weng, "Simulating the impacts of future land use and climate changes on surface water quality in the Des Plaines River watershed, Chicago Metropolitan Statistical Area, Illinois," *Science of the Total Environment*, vol. 409, no. 20, pp. 4387–4405, 2011.

[10] S. L. Ermida, P. Soares, V. Mantas, F. M. Göttsche, and I. F. Trigo, "Google earth engine open-source code for land surface temperature estimation from the landsat series," *Remote Sensing*, vol. 12, no. 9, pp. 1–21, 2020, doi: 10.3390/RS12091471.

[11] A. Maishella, B. E. B. Dewantoro, and M. A. P. Aji, "Correlation Analysis of Urban Development and Land Surface Temperature Using Google Earth Engine in Sleman Regency, Indonesia," *IOP Conference Series: Earth and Environmental Science*, vol. 540, p. 012018, 2020, doi: 10.1088/1755-1315/540/1/012018.

[12] N. Gorelick, M. Hancher, M. Dixon, S. Ilyushchenko, D. Thau, and R. Moore, "Google Earth Engine: Planetary-scale geospatial analysis for everyone," *Remote Sensing of Environment*, vol. 202, no. 2016, pp. 18–27, 2017, doi: 10.1016/j.rse.2017.06.031.

[13] H. Tamiminia, B. Salehi, M. Mahdianpari, L. Quackenbush, S. Adeli, and B. Brisco, "Google Earth Engine for geo-big data applications: A meta-analysis and systematic review," *ISPRS Journal of Photogrammetry and Remote Sensing*, vol. 164, no. January, pp. 152–170, 2020, doi: 10.1016/j.isprsjprs.2020.04.001.

[14] T. Mugiraneza, A. Nascetti, and Y. Ban, "Continuous monitoring of urban land cover change trajectories with landsat time series and landtrendr-google earth engine cloud computing," *Remote Sensing*, vol. 12, no. 18, 2020, doi: 10.3390/RS12182883.

[15] V. Matthies, "The 'Spirit of Bandung' 1955-1985: Thirty years since the Bandung Conference," *Intereconomics*, vol. 20, no. 5, pp. 207–210, 1985, doi: 10.1007/BF02926965.

[16] Q. Weng, D. Lu, and J. Schubring, "Estimation of land surface temperature-vegetation abundance relationship for urban heat island studies," *Remote Sensing of Environment*, vol. 89, no. 4, pp. 467–483, 2004, doi: 10.1016/j.rse.2003.11.005.

[17] A. Tariq *et al.*, "Land surface temperature relation with normalized satellite indices for the estimation of spatio-temporal trends in temperature among various land use land cover classes of an arid Potohar region using Landsat data," *Environmental Earth Sciences*, vol. 79, no. 1, pp. 1–15, 2020, doi: 10.1007/s12665-019-8766-2.

[18] U.S. Geological Survey, "Landsat 8 Data Users Handbook," *Nasa*, vol. 8, no. June, p. 97, 2016.

[19] "Landsat 8 (L8) Data Users Handbook," 2019.

[20] C. J. Tucker, "Red and photographic infrared linear combinations for monitoring vegetation," *Remote Sensing of Environment*, vol. 8, no. 2, pp. 127–150, 1979, doi: 10.1016/0034-4257(79)90013-0.

[21] F. Mukherjee and D. Singh, "Assessing Land Use–Land Cover Change and Its Impact on Land Surface Temperature Using LANDSAT Data: A Comparison of Two Urban Areas in India," *Earth Systems and Environment*, vol. 4, no. 2, pp. 385–407, 2020, doi: 10.1007/s41748-020-00155-9.

[22] A. S. Hope and T. P. McDowell, "The relationship between surface temperature and a spectral vegetation index of a tallgrass prairie: Effects of burning and other landscape controls," *International Journal of Remote Sensing*, vol. 13, no. 15, pp. 2849–2863, 1992, doi: 10.1080/01431169208904086.

[23] M. Wang *et al.*, "A radiance-based split-window algorithm for land surface temperature retrieval: Theory and application to MODIS data," *International Journal of Applied Earth Observation and Geoinformation*, vol. 76, no. April, pp. 204–217, 2019, doi: 10.1016/j.jag.2018.11.015.

[24] T. N. Carlson and D. A. Ripley, "On the relation between NDVI, fractional vegetation cover, and leaf area index," *Remote Sensing of Environment*, vol. 62, no. 3, pp. 241–252, 1997, doi: 10.1016/S0034-4257(97)00104-1.

[25] S. Pal and S. Ziaul, "Detection of land use and land cover change and land surface temperature in English Bazar urban centre," *Egyptian Journal of Remote Sensing and Space Science*, vol. 20, no. 1, pp. 125–145, 2017, doi: 10.1016/j.ejrs.2016.11.003.

[26] B. OS and A. AA, "Change Detection in Land Surface Temperature and Land Use Land Cover over Lagos Metropolis, Nigeria.," *Journal of Remote Sensing & GIS*, vol. 5, no. 3, 2016, doi: 10.4172/2469-4134.1000171.

[27] L. Chen, M. Li, F. Huang, and S. Xu, "Relationships of LST to NDBI and NDVI in Changsha-Zhuzhou-Xiangtan area based on MODIS data," *6th International Congress on Image and Signal Processing (CISP 2013)*, no. Cisp, pp. 840–845, 2013.

[28] O. Adeola Fashae, E. Gbenga Adagbasa, A. Oludapo Olusola, and R. Oluseyi Obateru, "Land use/land cover change and land surface temperature of Ibadan and environs, Nigeria," *Environmental Monitoring and Assessment*, vol. 192, no. 2, 2020, doi: 10.1007/s10661-019-8054-3.

[29] W. K. Boediono, "Teori dan aplikasi statistika dan probabilitas," *Bandung: Remaja Rosdakarya*, 2001.

[30] R. G. Congalton, "A review of assessing the accuracy of classifications of remotely sensed data," *Remote sensing of environment*, vol. 37, no. 1, pp. 35–46, 1991.